

Accelerated Luminophore Discovery through Combinatorial Synthesis

Michael S. Lowry, William R. Hudson, Robert A. Pascal, Jr., and Stefan Bernhard*

Contribution from the Department of Chemistry, Princeton University, Frick Laboratory, Princeton, New Jersey 08544

Received May 14, 2004; E-mail: sbernar@princeton.edu

Abstract: A method for accelerating the discovery of ionic luminophores using combinatorial techniques is reported. The photophysical properties of the resulting transition-metal-based chromophores were compared against a series of analogous, traditionally prepared species. The strong overlap between these two sets confirms the identity of the parallel synthesis products and supports the truthfulness of the combinatorial results. Further support for the combinatorial method comes from the adherence of these complexes to the energy gap law. The relationship between the structure of a complex and its photophysical properties was also considered, and static DFT calculations were used to assess whether it is feasible to predict the luminescent behavior of novel materials.

Introduction

Ionic transition-metal complexes have emerged as promising candidates for applications in solid-state electroluminescent devices. These materials serve as multifunctional chromophores, into which electrons and holes are injected and then migrate and recombine to exhibit light emission.^{1–6} In particular, transition-metal complexes are appealing luminescent materials because their properties (and net charge) can be tuned through ligation, thereby enabling facile, synthetic control over device performance. Consequently, the design of novel complexes for OLED applications has become a chief synthetic goal in materials research.^{7–9}

The usefulness and applicability of new luminescent materials can be assessed according to their stability, external quantum yield, excited-state lifetime, and emission energy. It is highly desirable to tailor transition-metal complexes that will emit across the visible spectrum and to produce molecules in which light emission predominates over nonradiative decay. These properties can be evaluated using both photo- and electroluminescent methods.

There are three electrochemical stages associated with light emission in a diode-type device: (1) charge injection, (2) charge transport, and (3) electron–hole recombination.^{10,11} Although OLEDs operate through electron-induced emission, solution-based photoluminescence studies provide a simple means of modeling and examining the radiative pathways in new materials and, thus, can be used to optimize their photophysical properties.

The majority of ionic chromophores that have been studied for single-layer devices involve osmium(II),¹² ruthenium(II),^{1–6,13} and rhenium(I).^{14,15} These materials emit primarily in the orange-red portion of the spectrum (600–650 nm) and have shown little sign of improvement with respect to color-tunability. Recently, however, Slinker et al. observed efficient yellow electroluminescence from a single-layer of a mixed-ligand iridium(III) complex, [Ir(ppy)₂(dtbbpy)](PF₆) (where ppy = 2-phenylpyridine; dtbbpy = 4,4'-di-*tert*-butyl-2,2'-dipyridyl), marking the highest emission energy from a single-layer device, to date.¹⁶

Because of its success, it is important to consider Slinker et al.'s complex more intimately. The dtbbpy-complex has a higher emission energy, a longer lifetime, and better photo- and electroluminescent quantum yields than does its more thoroughly investigated parent complex, [Ir(ppy)₂(bpy)](PF₆).^{16–19} Although a systematic relationship between photo- and electrolumines-

- (1) Slinker, J.; Bernards, D.; Houston, P. L.; Abruña, H. D.; Bernhard, S.; Malliaras, G. G. *Chem. Commun.* **2003**, 2392–2399.
- (2) Gao, F. G.; Bard, A. J. *J. Am. Chem. Soc.* **2000**, *122*, 7426–7427.
- (3) Rudmann, H.; Shimada, S.; Rubner, M. F. *J. Am. Chem. Soc.* **2002**, *124*, 4918–4921.
- (4) Buda, M.; Kalyuzhny, G.; Bard, A. J. *J. Am. Chem. Soc.* **2002**, *124*, 6090–6098.
- (5) Bernhard, S.; Barron, J. A.; Houston, P. L.; Abruña, H. D.; Ruglovsky, J. L.; Gao, X.; Malliaras, G. G. *J. Am. Chem. Soc.* **2002**, *124*, 13624–13628.
- (6) Lamansky, S.; Djurovich, P.; Murphy, D.; Abdel-Razzaq, F.; Kwong, R.; Tsyba, I.; Bortz, M.; Mui, B.; Bau, R.; Thompson, M. E. *Inorg. Chem.* **2001**, *40*, 1704–1711.
- (7) Lamansky, S.; Djurovich, P.; Murphy, D.; Abdel-Razzaq, F.; Lee, H. E.; Adachi, C.; Burrows, P.; Forrest, S. R.; Thompson, M. E. *J. Am. Chem. Soc.* **2001**, *123*, 4304–4312.
- (8) Pohl, R.; Montes, V. A.; Shinar, J.; Pavel Anzenbacher, J. *J. Org. Chem.* **2004**, *69*, 1723–1725.
- (9) Tsuboyama, A.; Iwawaki, H.; Furugori, M.; Mukaide, T.; Kamatani, J.; Igawa, S.; Moriyama, T.; Miura, S.; Takiguchi, T.; Okada, S.; Hoshino, M.; Ueno, K. *J. Am. Chem. Soc.* **2003**, *125*, 12971–12979.

- (10) Forrest, S.; Burrows, P.; Thompson, M. *IEEE Spectrum* **2000**, 29–34.
- (11) Tang, C. W.; VanSlyke, S. A. *Appl. Phys. Lett.* **1987**, *51*, 913–915.
- (12) Bernhard, S.; Gao, X.; Malliaras, G. G.; Abruña, H. D. *Adv. Mater.* **2002**, *14*, 433–436.
- (13) Reveco, P.; Schmehl, R. H.; Cherry, W. R.; Fronczek, F. R.; Selbin, J. *Inorg. Chem.* **1985**, *24*, 4078–4082.
- (14) Gong, X.; Ng, P. K.; Chan, W. K. *Adv. Mater.* **1998**, *10*, 1337–1340.
- (15) Spellane, P.; Watts, R. J.; Vogler, A. *Inorg. Chem.* **1993**, *32*, 5633–5636.
- (16) Slinker, J. D.; Gorodetsky, A. A.; Lowry, M. S.; Wang, J.; Parker, S.; Rohl, R.; Bernhard, S.; Malliaras, G. G. *J. Am. Chem. Soc.* **2004**, *126*, 2763–2767.
- (17) Wilde, A. P.; Watts, R. J. *J. Phys. Chem.* **1991**, *95*, 622–629.
- (18) Colombo, M. G.; Güdel, H. U. *Inorg. Chem.* **1993**, *32*, 3081–3087.
- (19) Colombo, M. G.; Hauser, A.; Güdel, H. U. *Inorg. Chem.* **1993**, *32*, 3088–3092.

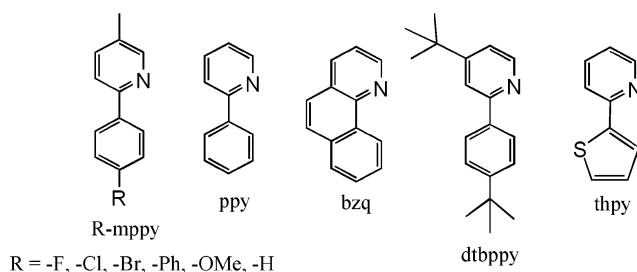
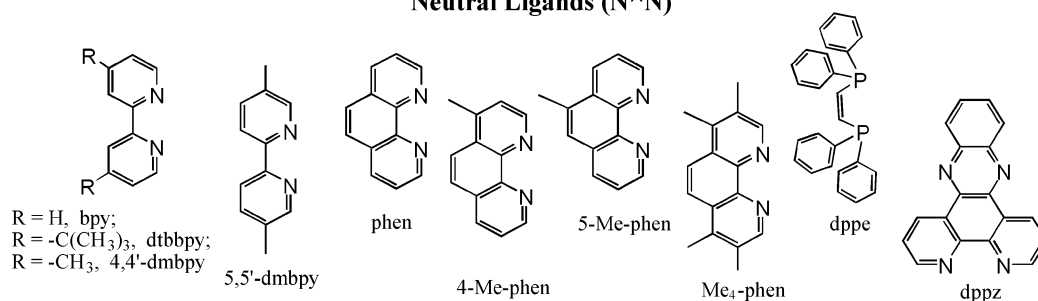
Cyclometalating Ligands (C \wedge N)Neutral Ligands (N \wedge N)

Figure 1. Ten cyclometalating (C \wedge N) and 10 neutral (N \wedge N) ligands.

cence in solid-state devices has yet to be revealed, improved photoluminescence appears to be a good predictor of improved luminescence in electronic devices. It is currently believed that such a relationship will persist for similar ligand systems. Moreover, the source of these differences in luminescent properties — a function of their chemical structure — is not yet well understood and needs to be addressed. It is important, therefore, to synthesize a large series of structurally similar, noncongruent complexes to assess the impact of chemical modifications on the photophysical properties of multifunctional chromophores.

As the effect of ligation on luminescent behavior becomes better understood, it will become possible to predict the properties of light emission for a novel complex from its structural design. Yet, before any intelligent predictions can be made, the number of luminescent compounds whose photophysical properties are well-established must be dramatically increased. Expansion of the known library of luminescent molecules is limited by the time and effort required to synthesize, purify, and characterize each individual complex by traditional synthetic methods. The introduction of combinatorial chemistry to this class of research is extremely appealing because it can be used to expedite the production of a molecularly diverse library of compounds.

In the present investigation, a library of 100 complexes has been prepared by coordinating one neutral, diimine and two equivalent cyclometalating (C \wedge N) ligands to an iridium(III) metal center, [Ir(C \wedge N)₂(N \wedge N)]Cl. By simultaneously and independently varying these two ligand groups, it is possible to monitor photophysical changes as a function of ligand structure in the coordination sphere. The compounds in this library were synthesized using 10 cyclometalating and 10 diimine-type ligands (Figure 1) [where C \wedge N = ppy, benzo[*h*]-quinoline (bhq), 2-thienylpyridine (thpy), 4,5'-di-*tert*-butyl-2-phenylpyridine (dtbppy), and six 5-methyl-2-(4-“R”-phenyl)-pyridines (R-mppy); and N \wedge N = bpy, dtbppy, 4,4'-di-methyl-2,2'-dipyridyl (4,4'-dmbpy), 5,5'-di-methyl-2,2'-dipyridyl (5,5'-

dmbpy), 1,10-phenanthroline (phen), 4-methyl-1,10-phenanthroline (4-Me-phen), 5-methyl-1,10-phenanthroline (5-Me-phen), 3,4,7,8-tetra-methyl-1,10-phenanthroline (Me₄-phen), bis-(diphenylphosphino)ethylene (dppe), and dipyriddyphenazine (dppz)]. A parallel synthetic approach was employed, and photophysical properties were measured directly from the reaction mixtures. The effectiveness of this methodology was assessed by comparing the resulting photophysical data to the data that were obtained for a small subset of analogous complexes prepared by traditional methods. Efforts to relate the structure of a given complex to its luminescent behavior using static DFT calculations were also considered and are presented below.

Experimental Section

One hundred iridium(III) and 10 ruthenium(II) complexes were synthesized using parallel synthetic techniques, and 11 control complexes were prepared using traditional methods. A generic reaction scheme for the synthesis of mixed-ligand iridium(III) complexes is presented in Figure 2. All solvents and reagents for these procedures were purchased from Aldrich and used without further purification.

Synthesis of Tetrakis-(C \wedge N)- μ -(dichloro)-diiridium(III). Stoichiometric quantities of the appropriate cyclometalating ligand (ligand synthesis is described in the Supporting Information) were added to a mixture of iridium chloride trihydrate hydrochloride in a methoxyethanol:water (5:1) solution. The reaction vessel was heated under reflux (120 °C) with constant stirring for 12 h. The resulting precipitate was collected by suction filtration, washed with water and diethyl ether, and dried to yield the product, [(C \wedge N)₂Ir- μ -Cl]₂ (yield: 72–85%).

Synthesis of Control Complexes (“Traditional Synthesis”): [(N \wedge N)-Bis-(C \wedge N)-iridium(III)] Hexafluorophosphate. The dichloro-bridged dimer (0.1 mmol) was permitted to react with the appropriate neutral ligand (0.22 mmol) in ethylene glycol (5.0 mL) under reflux (150 °C) with constant stirring for 15 h. Upon cooling to room temperature, the mixture was transferred to a separatory funnel with water (3 \times 30 mL) and washed with diethyl ether (3 \times 50 mL) (except in the case of C \wedge N = dtbppy where hexanes (3 \times 50 mL) were used to wash the mixture). The aqueous layer was heated to 70 °C for 5 min using a heat gun to remove residual organic solvents. The vessel was then placed on ice, and 10 mL of aqueous ammonium hexafluoro-

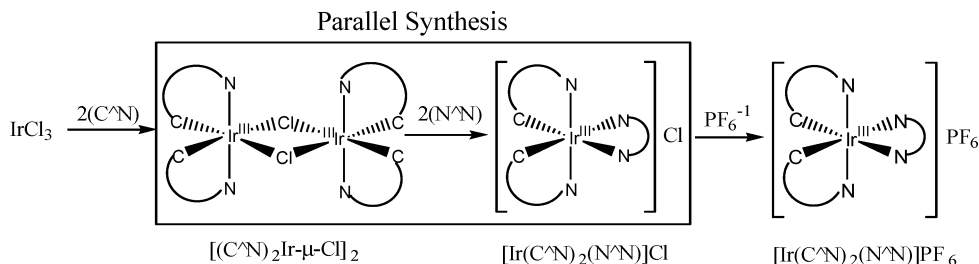


Figure 2. Synthetic pathway for the preparation of ionic iridium(III) chromophores. The boxed portion of the figure represents the step that is explored through parallel synthesis.

rophosphate solution (1.0 g in 10 mL of deionized water) was slowly added to the reaction mixture, yielding a colored suspension. The precipitate was collected by suction filtration and allowed to air-dry overnight. This product was recrystallized by acetonitrile:diethyl ether vapor diffusion (except for $\text{C}^{\wedge}\text{N} = \text{dtbppy}$, where hexane:acetone vapor diffusion was used instead) and dried in vacuo (100 °C) for 24 h to yield the pure product, $[\text{Ir}(\text{C}^{\wedge}\text{N})_2(\text{N}^{\wedge}\text{N})](\text{PF}_6)$ (yield: 68–80%).

Structural Identification. Structures for the 11 traditional synthesis products were confirmed using NMR and MS data. A Varian Inova-500 spectrometer was used to collect all ^1H and ^{13}C NMR spectra. A Hewlett-Packard 5898B (Electrospray) MS Engine was used to measure the mass spectra. These results are summarized in the Supporting Information.

Parallel Synthesis Protocol: [(N^N)-Bis-(C^N)-iridium(III)] Chloride. Homogeneous stock solutions of “n” iridium dichloro-bridged dimers [4 mM] were prepared in ethylene glycol, and stock solutions of “m” neutral ligands [8 mM; $\text{N}^{\wedge}\text{N}$] were prepared in acetonitrile. In each of the ($n \times m$) reaction vessels (medium test tubes), 250 μL of the appropriate dimer solution (0.001 mmol) was reacted with 270 μL of neutral ligand solution (0.0022 mmol) in ethylene glycol (750 μL) at 150 °C for 15 h to give the product, $[\text{Ir}(\text{C}^{\wedge}\text{N})_2(\text{N}^{\wedge}\text{N})]\text{Cl}$. Upon cooling to room temperature, all ($n \times m$) products were available for screening and spectroscopic characterization.

Parallel Synthesis of [Ruthenium(II) tris-(N^N)] Dichloride Complexes. Homogeneous stock solutions of ruthenium(III) chloride [1 mM, ethylene glycol] and the 10 neutral ligands [8 mM, acetonitrile] were prepared. The metal solution (1.0 mL, 0.001 mmol) reacted with the appropriate ligand solution (337 μL , 0.0033 mmol) at 150 °C for 15 h to give the product, $[\text{Ru}(\text{N}^{\wedge}\text{N})_3]\text{Cl}_2$. Upon cooling to room temperature, all 10 products were available for screening and spectroscopic characterization.

Screening and Photophysical Characterization. UV spectra were recorded at room temperature in a 1.0 cm quartz cuvette using a Hewlett-Packard 8453 spectrometer equipped with a diode-array detector.

Emission spectra were recorded using a Jobin-Yvon Fluorolog-3 spectrometer equipped with double monochromators and a Hamamatsu-928 photomultiplier tube (PMT) as the detector. Front face detection was used for the combinatorial experiments, and right angle detection was used for the control experiments. All complexes were excited at 400 nm (except for members of the dppe-series, which were excited at 360 nm). All emission spectra were adjusted according to the calibrated correction factors of the instrument.

Excited-state lifetimes were measured using the emission monochromator and PMT detector of the Jobin-Yvon Fluorolog-3 spectrometer. The samples were excited at 337 nm with an N_2 laser (Laser Science, Inc. VSL-337LRF, 10 ns pulse), and the emission decay was recorded using a Tektronix TDS 3032B digital phosphor oscilloscope.

Sample Preparation: Parallel Synthesis. All 110 samples were diluted with 5.0 mL of acetonitrile, the reaction vessels were sealed with rubber septa, and the samples were degassed with nitrogen for 10 min prior to emission and excited-state lifetime analyses. These parameters were measured directly from the reaction vessel. The

reaction mixtures were subsequently diluted with 10.0 mL of acetonitrile and transferred to a 1.0 cm quartz cuvette for the collection of absorption data.

Traditional Synthesis. Solutions of each monomeric complex [25 μM] were prepared in acetonitrile. Aliquots of each solution were transferred to a 1.0 cm capped quartz cuvette and degassed with nitrogen for 10 min before measuring their emission, absorption, and excited-state lifetime.

Quantum Yield. The emission quantum yield (Φ_{em}) was calculated for each complex according to the equation:²⁰

$$\Phi_s = \Phi_r \cdot (I_s/I_r) \cdot (A_r/A_s) \quad (1)$$

where Φ_s is the quantum yield of the sample, A_s and A_r are the absorbance of the sample and the reference at the excitation wavelength, and I_s and I_r represent the points of maximum intensity in the corrected emission spectra. Φ_r is the quantum yield for the reference complex; $[\text{Ru}(\text{bpy})_3](\text{PF}_6)_2$ ($\Phi = 6.20\%$) is the reference for the control products, $[\text{Ir}(\text{ppy})_2(\text{bpy})]\text{Cl}$ ($\Phi = 6.22\%$) is the reference for the parallel synthesis products, and $[\text{Ru}(\text{bpy})_3]\text{Cl}_2$ ($\Phi = 6.20\%$) is the reference for the ruthenium combinatorial products.^{1–6}

Computational Studies. Hybrid density functional calculations (B3LYP/LANL2DZ) were performed by using Gaussian 98.²¹ The built-in default thresholds for gradient convergence were employed, but the threshold for wave function convergence was slightly relaxed [SCF=(CONVER=7)]. All geometry optimizations were carried out under the constraint of C_2 symmetry.

Results and Discussion

Ligand Synthesis. Five novel cyclometalating ligands ($\text{C}^{\wedge}\text{N} = \text{dtbppy}$, F-mppy, Cl-mppy, Br-mppy, Ph-mppy) were synthesized. Each of these five new systems was prepared by following a modified literature procedure, utilizing either the Kröhnke pyridine synthesis²² (“R”-mppy) or the Suzuki coupling reaction (dtbppy).^{23,24} Details for the synthesis and characterization of these systems are described in the Supporting Information.

- (20) Parker, C. A. *Measurement of Fluorescence Efficiency*; Elsevier Publishing Co.: New York, 1968; pp 261–269.
- (21) Frisch, M. J.; Trucks, G. W.; Schlegel, H. B.; Scuseria, G. E.; Robb, M. A.; Cheeseman, J. R.; Zakrzewski, V. G.; Montgomery, J. A., Jr.; Stratmann, R. E.; Burant, J. C.; Dapprich, S.; Millam, J. M.; Daniels, A. D.; Kudin, K. N.; Strain, M. C.; Farkas, O.; Tomasi, J.; Barone, V.; Cossi, M.; Cammi, R.; Mennucci, B.; Pomelli, C.; Adamo, C.; Clifford, S.; Ochterski, J.; Petersson, G. A.; Ayala, P. Y.; Cui, Q.; Morokuma, K.; Malick, D. K.; Rabuck, A. D.; Raghavachari, K.; Foresman, J. B.; Cioslowski, J.; Ortiz, J. V.; Baboul, A. G.; Stefanov, B. B.; Liu, G.; Liashenko, A.; Piskorz, P.; Komaromi, I.; Gomperts, R.; Martin, R. L.; Fox, D. J.; Keith, T.; Al-Laham, M. A.; Peng, C. Y.; Nanayakkara, A.; Gonzalez, C.; Challacombe, M.; Gill, P. M. W.; Johnson, B.; Chen, W.; Wong, M. W.; Andres, J. L.; Gonzalez, C.; Head-Gordon, M.; Replogle, E. S.; Pople, J. A. *Gaussian 98*; Gaussian, Inc.: Pittsburgh, PA, 1998.
- (22) Gianini, M.; Forster, A.; Haag, P.; von Zelewsky, A.; Stoekli-Evans, H. *Inorg. Chem.* **1996**, *35*, 4889–4895.
- (23) Ali, N. M.; McKillop, A.; Mitchell, M. B.; Tebello, R. A.; Wallbank, P. J. *Tetrahedron* **1992**, *48*, 8117–8126.
- (24) Watanabe, T.; Miyaura, N.; Suzuki, A. *Synlett* **1992**, 207–210.

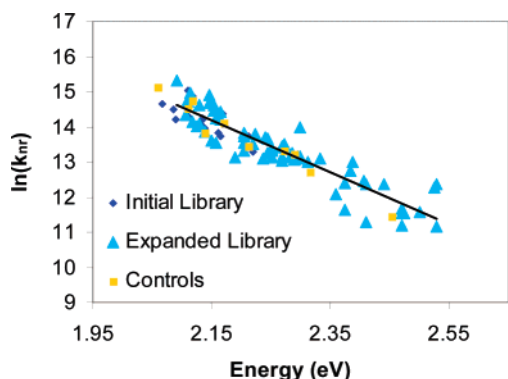


Figure 3. An application of the energy gap law to the compounds that were prepared in the initial subset and in the full expanded library. The matching linear trends for the subset and the expanded library as well as their close correlation to the 11 control points suggest that the complexes have been accurately prepared and consistently measured.

Evaluating the Combinatorial Approach. A subset of 24 complexes from the 100-member iridium(III) library was initially prepared to examine the effectiveness of the combinatorial techniques. This subset was prepared using four cyclo-metallating ligands (ppy, dtbbpy, bhq, and thpy) and six neutral ligands (bpy, dtbbpy, 5,5'-dmbpy, phen, 4-Me-phen, 5-Me-phen); each of the resulting 24 iridium(III) complexes was characterized for its emission energy, quantum yield, and excited-state lifetime. The results of these analyses were considered with respect to their adherence to the energy gap law and their closeness to the values obtained from five analogous control complexes.

An energy gap plot (Figure 3) was prepared for these 24 complexes (and later extended to include the rest of the library) by plotting the natural log of the nonradiative decay rate constant (k_{nr}) as a function of emission energy. The value of k_{nr} can be calculated according to the equation:²⁵

$$k_{nr} = 1/\tau - k_r = [(1 - \Phi_{em})/\tau] \quad (2)$$

where the radiative rate constant (k_r) is equal to the ratio of the quantum yield over the emission lifetime (τ , in s). Because all three relevant photophysical parameters are taken into account, conformity to the energy gap law (a linear plot with negative slope) suggests that the data have been consistently and accurately measured. Perhaps equally important, it is easy to identify which reaction mixtures and measurements are inconsistent by locating outliers in the plot.²⁵

Along these lines, the thpy-series had to be excluded from the initial subset because it did not follow the same linear trend as the other 18 data points. It is currently hypothesized that the reaction of $[(\text{thpy})_2\text{Ir}-\mu\text{-Cl}]_2$ with a neutral ligand does not yield the desired product under the given combinatorial conditions. The relatively constant emission energy of these complexes (592 nm) across different N \wedge N ligands as well as the small Stokes shift exhibited by the thpy-series suggests that a fluorescent byproduct of the reaction is being probed rather than the desired target complex.

The remaining 18 complexes obey the energy gap law, demonstrating a linear relationship that perfectly corresponds with the five controls. This matching relationship implies that

the measured emission energy, quantum yield, and excited-state lifetime are approximately the same regardless of which method was used to prepare the luminophore and that parallel synthesis is viable for the production of transition-metal complexes.

The library was subsequently expanded to include 76 new mixed-ligand iridium(III) complexes and 10 tris-diimine ruthenium(II) complexes; six additional control species were also prepared. To confirm that there were no systematic errors between the initial subset and the expanded library, an internal standard, $[\text{Ir}(\text{ppy})_2(\text{dtbbpy})]\text{Cl}$, was synthesized and characterized both times. The emission maxima ($\lambda = 570 \text{ nm}$, 570 nm), corrected quantum yields ($\Phi_{em} = 17.51\%$, 17.89%), and excited-state lifetimes ($\tau = 617 \text{ ns}$, 621 ns) are extremely close and are consistent with the values reported by Slinker et al. for the pure, PF_6^- -salt of this complex.¹⁶

To construct an energy gap plot for the expanded library, the thpy-series and the dppz-series had to be excluded. As was the case for the initial subset, the thpy-complexes were eliminated because they constantly fluoresced at a single energy across multiple N \wedge N ligands. Similarly, the members of the strongly absorbing dppz-series could not be included because their excited states were too short-lived to be measured by our instrument. A plot featuring the remaining 81 iridium(III) complexes shows that the library conforms to the energy gap law and that the new data are consistent with the first subset. A matching linear relationship was also observed for the control complexes (Figure 3).

The normalized absorption and emission spectra of the complexes in the expanded library closely match those of the controls. These strong spectral similarities (e.g., band-shapes and emission maxima) suggest that the appropriate complexes were prepared during the parallel synthesis. Examples of overlaid spectra are presented in the Supporting Information. A summary of the photophysical properties for the control complexes with their corresponding combinatorial products is presented in Table 1. It is worth noting that the use of different counterions (Cl^- vs PF_6^-) and slightly different solvent systems between the combinatorial and traditional methods did not significantly impact these results.

Photophysical Observations. As can be seen in Table 1, a broad range of values were revealed for the emission energy, quantum yield, and excited-state lifetime of the complexes in the expanded library. Three-dimensional plots of these properties for the complete library are shown in Figure 4. Due to the order of magnitude deviations between the highest and lowest lifetime, these values were plotted on a logarithmic scale. The results for all 110 complexes are tabulated in the Supporting Information.

Perhaps the most intriguing observation was the color versatility expressed by the complexes in this library (Figure 4). The emission maxima spanned from blue for the dppe-series (450 nm) to red-orange (615 nm) for the ruthenium(II)-series with corrected photoluminescent yields ranging from 0.02% to 32.01% and lifetimes that span from nano- to microseconds. Such properties will be extremely useful for introducing the visible spectrum to single-layer, ionic OLED displays. A collection of novel luminophores were targeted from this library for their interesting photophysical properties and have been tested in optoelectronic devices. These results will be reported in a future publication.²⁶

(25) Kalyanasundaram, K.; *Photochemistry of Polypyridine and Porphyrin Complexes*; Academic Press: New York, 1992; pp 172–173.

Table 1. A Comparison of the Photophysical Properties of the Products from the Expanded Library (Cl^-) and Their Analogous Controls (PF_6^-)^a

sample complex	Cl^-	PF_6^-
$[\text{Ir}(\text{ppy})_2(\text{bpy})]^+1$ $\lambda = 583 \text{ nm}$	$\Phi = 6.22 \pm 0.28\%$ $\tau = 329 \pm 13 \text{ ns}$	$\Phi = 7.07 \pm 0.39\%$ $\tau = 269 \pm 11 \text{ ns}$
$[\text{Ir}(\text{ppy})_2(\text{dtbbpy})]^+1$ $\lambda = 570 \text{ nm}$	$\Phi = 17.89 \pm 0.82\%$ $\tau = 495 \pm 20 \text{ ns}$	$\Phi = 17.16 \pm 1.10\%$ $\tau = 621 \pm 25 \text{ ns}$
$[\text{Ir}(\text{dtbbpy})_2(\text{bpy})]^+1$ $\lambda = 597 \text{ nm}$	$\Phi = 4.66 \pm 0.21\%$ $\tau = 424 \pm 17 \text{ ns}$	$\Phi = 4.46 \pm 0.20\%$ $\tau = 258 \pm 11 \text{ ns}$
$[\text{Ir}(\text{dtbbpy})_2(\text{dtbbpy})]^+1$ $\lambda = 583 \text{ nm}$	$\Phi = 11.84 \pm 0.54\%$ $\tau = 389 \pm 16 \text{ ns}$	$\Phi = 9.47 \pm 0.47\%$ $\tau = 444 \pm 18 \text{ ns}$
$[\text{Ir}(\text{ppy})_2(5,5'\text{-dmbpy})]^+1$ $\lambda = 558 \text{ nm}$	$\Phi = 20.12 \pm 0.92\%$ $\tau = 877 \pm 36 \text{ ns}$	$\Phi = 20.53 \pm 0.94\%$ $\tau = 1166 \pm 48 \text{ ns}$
$[\text{Ir}(\text{ppy})_2(\text{phen})]^+1$ $\lambda = 577 \text{ nm}$	$\Phi = 12.49 \pm 0.78\%$ $\tau = 685 \pm 28 \text{ ns}$	$\Phi = 12.11 \pm 0.55\%$ $\tau = 877 \pm 36 \text{ ns}$
$[\text{Ir}(\text{ppy})_2(\text{Me}_4\text{-phen})]^+1$ $\lambda = 534 \text{ nm}$	$\Phi = 27.96 \pm 1.28\%$ $\tau = 1604 \pm 66 \text{ ns}$	$\Phi = 37.68 \pm 3.17\%$ $\tau = 1866 \pm 77 \text{ ns}$
$[\text{Ir}(\text{F-mppy})_2(\text{dtbbpy})]^+1$ $\lambda = 543 \text{ nm}$	$\Phi = 26.99 \pm 2.05\%$ $\tau = 1080 \pm 44 \text{ ns}$	$\Phi = 26.27 \pm 1.24\%$ $\tau = 1221 \pm 50 \text{ ns}$
$[\text{Ir}(\text{F-mppy})_2(\text{Me}_4\text{-phen})]^+1$ $\lambda = 506 \text{ nm}$	$\Phi = 28.15 \pm 1.29\%$ $\tau = 3026 \pm 124 \text{ ns}$	$\Phi = 44.99 \pm 4.70\%$ $\tau = 5884 \pm 241 \text{ ns}$
$[\text{Ir}(\text{Br-mppy})_2(\text{dtbbpy})]^+1$ $\lambda = 537 \text{ nm}$	$\Phi = 29.10 \pm 1.33\%$ $\tau = 1378 \pm 56 \text{ ns}$	$\Phi = 30.12 \pm 2.44\%$ $\tau = 1256 \pm 52 \text{ ns}$
$[\text{Ru}(\text{dtbbpy})_3]^{+2}$ $\lambda = 614 \text{ nm}$	$\Phi = 7.11 \pm 0.41\%$ $\tau = 980 \pm 40 \text{ ns}$	$\Phi = 6.29 \pm 0.30\%$ $\tau = 990 \pm 42 \text{ ns}$

^a These values are remarkably similar, and they support the notion that combinatorial results can be used as accurate predictors of the emission energy, quantum yield, and excited-state lifetime of pure, traditionally synthesized materials.

The development of such a structurally diverse library would have taken considerably longer using traditional methods, and, as such, we believe that the use of combinatorial chemistry will

rapidly become commonplace for accelerated luminoaphore discovery. The techniques that have been presented above will be of particular importance for continuing research with ionic, mixed-ligand iridium(III) systems and will also have extensions with different luminoaphore complexes. For instance, the neutral, heteroleptic iridium(III) complexes^{6,7} investigated by Thompson et al. can be prepared by following a similar synthetic pathway: A dichloro-bridged dimer is reacted with an ancillary ligand to yield the desired product.

The ruthenium(II) complexes that were prepared in the current library demonstrate the ability to apply this technique to other metals. The tris-N^N-series was selected for this study because of its agreement with the reaction conditions (ethylene glycol, 150 °C, 15 h), but the synthetic protocol could have easily been modified to accommodate a diverse range of solvents and reaction conditions. Other suitable candidates for this approach include rhenium(I),^{14,15,27,28} platinum(II),^{22,29,30} osmium(II),¹² and rhodium(III).^{31–33}

Excited-State Characteristics. ³MLCT and ³ π - π^* ligand-centered transitions are commonly observed in a vast majority of the presently investigated mixed-ligand transition-metal complexes. While it has been shown that there is a strong degree of mixing between these two emissive states in the $[\text{Ir}(\text{ppy})_2(\text{bpy})](\text{PF}_6)$ model,¹⁹ excited-state character has not been extensively studied with other ligand combinations. In $[\text{Ir}(\text{ppy})_2(\text{bpy})](\text{PF}_6)$, the ³MLCT transition arises from the promotion of an electron from a filled t_{2g} -orbital on the metal to a vacant π^* -orbital on the neutral, aromatic bpy-ligand. The ligand-

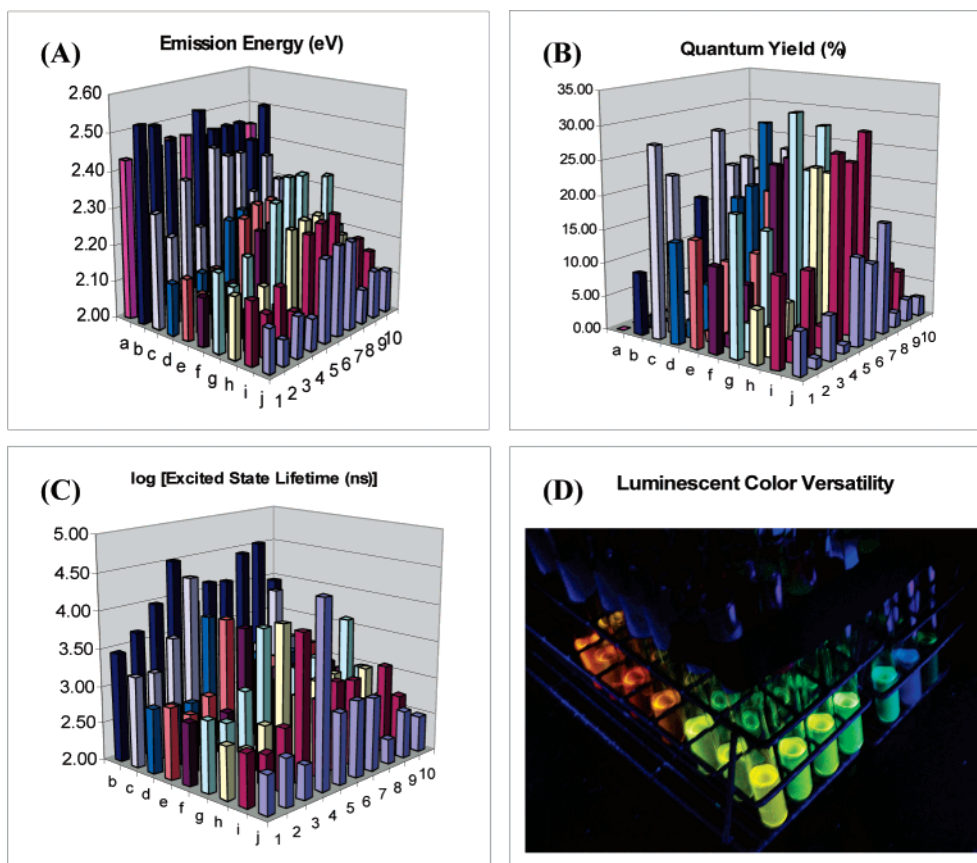


Figure 4. Three-dimensional plots for the (A) emission energy, (B) quantum yield, and (C) log(excited-state lifetime) for 100 iridium(III) complexes with the form $[\text{Ir}(\text{C}\wedge\text{N})_2(\text{N}\wedge\text{N})]\text{Cl}$. $\text{C}\wedge\text{N}$ = ppy (1), dtbbpy (2), bhq (3), thpy (4), F-mppy (5), Cl-mppy (6), Br-mppy (7), MeO-mppy (8), Ph-mppy (9), H-mppy (10). $\text{N}\wedge\text{N}$ = dpz (a), dppe (b), Me_4 -phen (c), 5-Me-phen (d), 4-Me-phen (e), phen (f), 5,5'-dmbpy (g), 4,4'-dmbpy (h), dtbbpy (i), bpy (j). As can be seen in panel (D), these complexes exhibit remarkable luminescent color versatility, spanning from blue to orange-red emission.

centered ${}^3\pi-\pi^*$ transition typically involves the movement of electrons between filled and vacant π -orbitals on the cyclometalating ppy-ligand.^{18,19,34}

To understand the photoluminescent properties of mixed systems, it is important to observe pure ${}^3\text{MLCT}$ and ${}^3\pi-\pi^*$ systems first. Thus, the ruthenium(II)- (containing only N \wedge N ligands) and dppe-complexes (containing no aromatic diimine ligands) were incorporated into the current library, respectively. All of the remaining complexes in the library have mixed excited states due to the presence of both cyclometalating and aromatic, diimine ligands. Trisubstituted ruthenium(II) was used in place of trisubstituted iridium(III) because the ruthenium complexes exhibit only ${}^3\text{MLCT}$ transitions, whereas their iridium analogues exhibit mixed-states with strong ${}^3\pi-\pi^*$ character.³² Moreover, the synthesis of the tris-diimine ruthenium species was also more compliant with the given reaction conditions.³³

From observation of the luminescence spectra of pure ${}^3\text{MLCT}$ and ${}^3\pi-\pi^*$ species, certain defining features become evident. For instance, the ${}^3\text{MLCT}$ emission bands tend to be broader and lower in energy than the vibrationally structured, blue-shifted ${}^3\pi-\pi^*$ bands. These spectral differences make it possible to assess the contribution of each transition-type to light emission in mixed-state systems. Although a quantitative method for describing the degree of mixing has yet to be determined, the current library shows us that this value is strongly ligand-dependent. The convolution of a mixed state from pure ${}^3\pi-\pi^*$ and ${}^3\text{MLCT}$ excited states is depicted in Figure 5.

By comparing the photophysical properties of the pure systems with those from the mixed-state systems, it further becomes clear that a simple correlation between the two does not exist. For instance, Figure 6 demonstrates the relationship between the emission energy of the pure transitions and their closest comparator from the mixed-state systems. These comparators were defined as the systems with the strongest spectral similarities to ruthenium(II) and dppe across all N \wedge N or C \wedge N variables (i.e., MeO-mppy was used for the ${}^3\text{MLCT}$ and Me₄-phen was used for the ${}^3\pi-\pi^*$). The nonlinear relationship between these data suggests that it may not be feasible to predict the luminescent properties of a mixed-state system through simple extrapolation from the pure excited-state materials and that a more convoluted interplay between these states exists. The electronic structure and orbital geometries of the ligands, as well as the manner in which those ligands interact with each other, dictate the emissive properties of the complex. Due to the fact that it is not a priori clear how these traits will be manifest in a given system, the study of a molecularly diverse

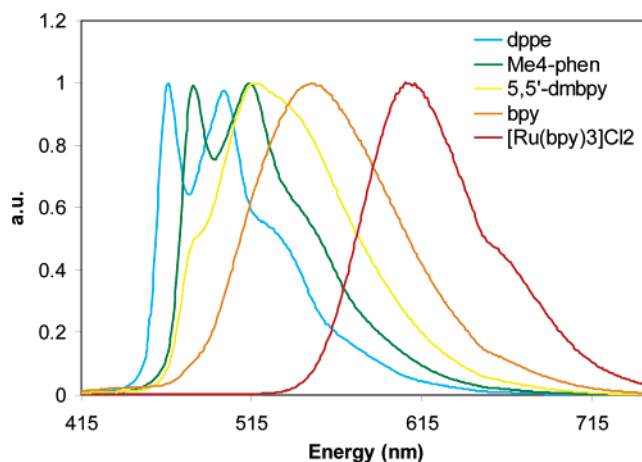


Figure 5. The evolution of a mixed excited state from ${}^3\pi-\pi^*$ (dppe) and ${}^3\text{MLCT}$ (ruthenium complex). The series shown represents the normalized emission spectra for a series of $[\text{Ir}(\text{Br-mppy})_2(\text{N}\wedge\text{N})]\text{Cl}$ complexes, where $\text{N}\wedge\text{N} = \text{dppe}$, $\text{Me}_4\text{-phen}$, $5,5'\text{-dmbpy}$, and bpy . $[\text{Ru}(\text{bpy})_3]\text{Cl}_2$ is included due to its strict ${}^3\text{MLCT}$ character. Changes in the character of the excited state can be monitored by the shape and position of the emission band, where blue-shifted dual bands are indicative of more ${}^3\pi-\pi^*$ character and a broad, red-shifted band suggests more ${}^3\text{MLCT}$ character.

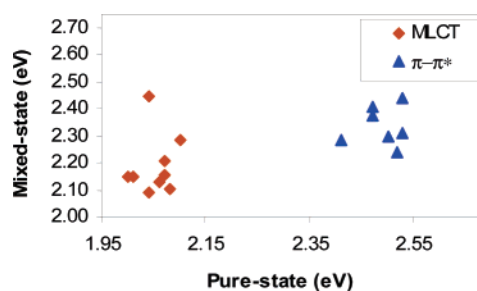


Figure 6. A comparison of the energy values obtained for the pure ${}^3\text{MLCT}$ Ru(II)-series (orange \blacklozenge) with its nearest mixed-state analogue (MeO-mppy), as well as for the pure ${}^3\pi-\pi^*$ dppe-series (blue \blacktriangle) with its nearest mixed-state analogue (Me₄-phen). As can clearly be seen in the plot, a simple correlation between the pure and the mixed state species does not exist.

library of such complexes is necessary, and no accurate predictions of structure–property relationships can currently be made.

Computational Prediction. To more efficiently plan future libraries, the measured emission maxima of selected complexes were correlated with energy differences obtained from static DFT calculations (B3LYP/LANL2DZ). The consistency of the spectroscopic measurements in the library facilitates such comparisons. Three different strategies were used on seven complexes with phosphorescence maxima ranging from 2.07 eV (600 nm) to 2.53 eV (487 nm). The fastest calculations involved the optimization of the singlet geometry of the complexes and the correlation of the HOMO–LUMO gap to the luminescence maxima. The assumption that the singlet–triplet splitting energy and the nuclear rearrangements are similar in this family of complexes was confirmed by the overall linear relationship depicted in Figure 7. The only exception is the $[\text{Ir}(\text{F-mppy})_2(\text{dppe})]^+$ complex, which exhibits a pure $\pi-\pi^*$ transition and is, therefore, likely to have a larger singlet–triplet splitting energy than the complexes with mixed excited states. In a second method, the triplet geometry was optimized, and the difference in the total energy of the triplet and singlet states at this geometry was correlated with the observed emission maxima. The third approach was based on the work by

- (26) Slinker, J. D.; Lowry, M.; Parker, S.; Bernhard, S.; Malliaras, G. G. manuscript in preparation.
 (27) Li, F.; Zhang, M.; Cheng, G.; Feng, J.; Zhao, Y.; Ma, Y.; Liu, S.; Shen, J. *Appl. Phys. Lett.* **2004**, *84*, 148–150.
 (28) Ranjan, S.; Lin, S.; Hwang, K.; Chi, Y.; Ching, W.; Liu, C. *Inorg. Chem.* **2003**, *42*, 1248–1255.
 (29) Brooks, J.; Yelizaveta, B.; Lamansky, S.; Djurovich, P. I.; Tsyba, I.; Bau, R.; Thompson, M. E. *Inorg. Chem.* **2002**, *41*, 3055–3066.
 (30) DePriest, J.; Zheng, G. Y.; Goswami, N.; Eichhorn, D. M.; Woods, C.; Rillema, D. P. *Inorg. Chem.* **2000**, *39*, 1955–1963.
 (31) Frei, G.; Zilian, A.; Raselli, A.; Güdel, H. U.; Burgi, H.-B. *Inorg. Chem.* **1992**, *31*, 4766–4773.
 (32) Ghizdavu, L.; von Zelewsky, A.; Stoekli-Evans, H. *Eur. J. Inorg. Chem.* **2001**, 993–1003.
 (33) Ghizdavu, L.; Kolp, B.; von Zelewsky, A.; Stoekli-Evans, H. *Eur. J. Inorg. Chem.* **1999**, 1271–1279.
 (34) Wilde, A. P.; King, K. A.; Watts, R. J. *J. Phys. Chem.* **1991**, *95*, 629–634.

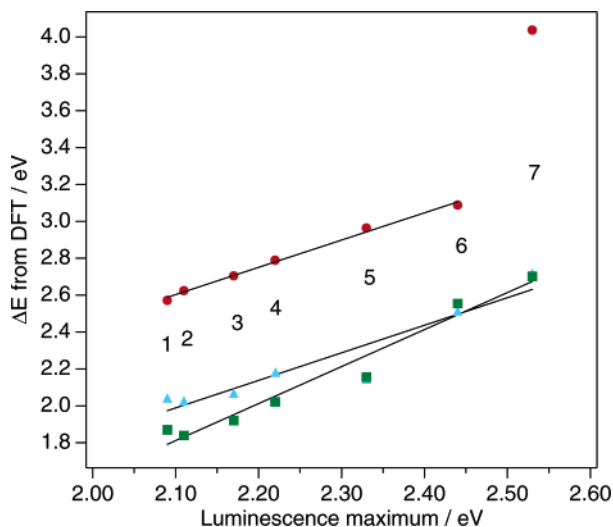


Figure 7. Correlation of the experimental luminescence maxima with the results of DFT calculations. Red ●: The HOMO–LUMO gap at optimized singlet geometry. Green ■: The difference of the absolute energy of the triplet configuration and the singlet configuration at the optimized triplet geometry. Blue ▲: The orbital energy difference of the HSOMO (triplet) and the HOMO (singlet) calculated at the triplet geometry. The data points represent the following: **1** [Ir(MeO-mppy)₂(bpy)]⁺, **2** [Ir(mppy)₂(bpy)]⁺, **3** [Ir(mppy)₂(4,4'-dmbpy)]⁺, **4** [Ir(F-mppy)₂(bpy)]⁺, **5** [Ir(F-mppy)₂(5,5'-dmbpy)]⁺, **6** [Ir(F-mppy)₂(Me₄-phen)]⁺, and **7** [Ir(F-mppy)₂(dppe)]⁺.

Thompson et al. in which the difference of the HOMO energy of the singlet and the highest singly occupied molecular orbital (HSOMO) energy of the triplet was used to predict the maxima.^{29,35} Again, both orbital energies were calculated at the optimized nuclear geometry of the triplet state. Data from the triplet state geometry optimization result in more consistent predictions, independent of the nature of the considered excited state.

Overall, static DFT calculations offer an acceptable prediction of the phosphorescence energy. However, no information regarding the excited-state lifetimes and phosphorescence quantum efficiency can be obtained from such DFT calculations. To this end, an adaptive substituent reordering algorithm is currently being explored that would interpolate the emission energy, quantum yield, and excited-state lifetime of new materials based on structure–property relationships.³⁶

Conclusion

The luminescent properties that were measured for this library of novel luminophores are astonishingly accurate considering that the products were analyzed directly from their reaction vessels without further workup or purification. The strong

coherence between the experimental data and the controls confirms that the appropriate complexes were prepared and that the photophysical properties of pure complexes can be predicted from their crude analogues. Thus, combinatorial methods will be extraordinarily useful for accelerating the discovery of luminophore complexes. Similarly, the use of combinatorial techniques will be economically shrewd and environmentally friendly because it will reduce the expenditure of resources while also dramatically decreasing the amount of waste generated during multiple syntheses.

From a materials science perspective, the combinatorial approach has proven to be a valuable tool for evaluating the relationship between ligand structure and emissive behavior. This technique is not limited to the arena of OLED discovery, however, and it may have extensions in a multitude of other scientific avenues. For instance, TiO₂-based photovoltaic cells,^{37–39} photoinduced water-splitting,^{40,41} biomolecular probes,^{42,43} and chiral luminophores^{44–46} all present intriguing opportunities for further exploration.

Acknowledgment. This work was supported in part by a Camille and Henry Dreyfus Foundation New Faculty Award, which is gratefully acknowledged. This work was partially supported by the NSF through grant DMR-0213706 to the MRSEC-Princeton Center for Complex Materials.

Supporting Information Available: Procedures for the synthesis of five novel cyclometallating ligands, seven dichloro-bridged diiridium(III) dimers, and nine iridium(III) hexafluorophosphate monomers. ¹H NMR chemical shifts, coupling constants, and peak identifications for all of the traditionally prepared species. ¹³C NMR and MS data for the traditionally prepared monomeric complexes. Normalized emission spectra for select library luminophores and their traditional analogues. Tables of emission energy, photoluminescent quantum yield, and excited-state lifetime for (n × m) complexes in the combinatorial library and 10 ruthenium(II) species. This material is available free of charge via the Internet at <http://pubs.acs.org>.

JA047156+

(35) Tamayo, A. B.; Alleyne, B. D.; Djurovich, P. I.; Lamansky, S.; Tsyba, I.; Ho, N. N.; Bau, R.; Thompson, M. E. *J. Am. Chem. Soc.* **2003**, *125*, 7377–7387.

(36) Liang, F.; Feng, X.; Lowry, M.; Bernhard, S.; Rabitz, H., manuscript in preparation.

(37) Hou, Y.; Xie, P.; Zhang, B.; Cao, Y.; Xiao, X.; Wang, W. *Inorg. Chem.* **1999**, *38*, 6320–6322.

(38) Anandan, S.; Latha, S.; Maruthamuthu, P. *J. Photochem. Photobiol., A* **2002**, *150*, 167–175.

(39) Mosurkal, R.; Kim, Y.; Kumar, J.; Li, L.; Walker, J.; Samuelson, L. A. *J. Macromol. Sci., Pure Appl. Chem.* **2003**, *A40*, 1317–1325.

(40) Harriman, A.; West, M. A. *Photogeneration of Hydrogen*; Academic Press: New York, 1982.

(41) Koelle, U. *New J. Chem.* **1992**, *16*, 157–169.

(42) Lo, K. K.; Chung, C.; Lee, T. K.; Lui, L.; Tsang, K. H.; Zhu, N. *Inorg. Chem.* **2003**, *42*, 6886–6897.

(43) Lo, K. K.; Chung, C.; Zhu, N. *Chem.-Eur. J.* **2003**, *9*, 475–483.

(44) Ghizdavu, L.; Lentzen, O.; Schumm, S.; Brodkorb, A.; Moucheron, O.; Kirsh-De Mesmaeker, A. *Inorg. Chem.* **2003**, *42*, 1935–1944.

(45) Ziegler, M.; von Zelewsky, A. *Coord. Chem. Rev.* **1998**, *177*, 257–300.

(46) Mürner, H.; Belsler, P.; von Zelewsky, A. *J. Am. Chem. Soc.* **1996**, *118*, 7989–7994.